

# **Afforestation for Reduction of NO<sub>x</sub> Concentration in Lanzhou China**

Peter C. Chu\*

Naval Ocean-Atmospheric Prediction Laboratory, Naval Postgraduate School,  
Monterey, California, USA

Yuchun Chen and Shihua Lu

Cold and Arid Regions Environmental and Engineering Research Institute, Chinese  
Academy of Sciences, Lanzhou, China

---

\*Corresponding author: Tel: +1-831-656-3688; Fax: +1-831-656-3686; E-mail address: pcchu@nps.edu  
URL: <http://www.oc.nps.navy.mil/~chu>

## Report Documentation Page

*Form Approved*  
*OMB No. 0704-0188*

Public reporting burden for the collection of information is estimated to average 1 hour per response, including the time for reviewing instructions, searching existing data sources, gathering and maintaining the data needed, and completing and reviewing the collection of information. Send comments regarding this burden estimate or any other aspect of this collection of information, including suggestions for reducing this burden, to Washington Headquarters Services, Directorate for Information Operations and Reports, 1215 Jefferson Davis Highway, Suite 1204, Arlington VA 22202-4302. Respondents should be aware that notwithstanding any other provision of law, no person shall be subject to a penalty for failing to comply with a collection of information if it does not display a currently valid OMB control number.

1. REPORT DATE <b>2008</b>	2. REPORT TYPE	3. DATES COVERED <b>00-00-2008 to 00-00-2008</b>			
4. TITLE AND SUBTITLE <b>Afforestation for Reduction of NOx Concentration in Lanzhou China</b>		5a. CONTRACT NUMBER			
		5b. GRANT NUMBER			
		5c. PROGRAM ELEMENT NUMBER			
6. AUTHOR(S)		5d. PROJECT NUMBER			
		5e. TASK NUMBER			
		5f. WORK UNIT NUMBER			
7. PERFORMING ORGANIZATION NAME(S) AND ADDRESS(ES) <b>Naval Postgraduate School, Department of Oceanography, Monterey, CA, 93943</b>		8. PERFORMING ORGANIZATION REPORT NUMBER			
9. SPONSORING/MONITORING AGENCY NAME(S) AND ADDRESS(ES)		10. SPONSOR/MONITOR'S ACRONYM(S)			
		11. SPONSOR/MONITOR'S REPORT NUMBER(S)			
12. DISTRIBUTION/AVAILABILITY STATEMENT <b>Approved for public release; distribution unlimited</b>					
13. SUPPLEMENTARY NOTES					
14. ABSTRACT					
15. SUBJECT TERMS					
16. SECURITY CLASSIFICATION OF:			17. LIMITATION OF ABSTRACT	18. NUMBER OF PAGES	19a. NAME OF RESPONSIBLE PERSON
a. REPORT <b>unclassified</b>	b. ABSTRACT <b>unclassified</b>	c. THIS PAGE <b>unclassified</b>	<b>Same as Report (SAR)</b>	<b>32</b>	

## **Abstract**

Lanzhou is one of the major industrial cities in northwest China, the capital of Gansu Province, and located at a northwest-to-southeast oriented valley basin with elevation about 1,500-1,600-m. Due to topographic and meteorological characteristics, Lanzhou is one of the most polluted cities in China. Meteorological conditions (low winds, stable stratification especially inversion), pollutant sources and sinks affect the air quality. Lanzhou government carried out afforestation and pollutant-source reduction (closing several heavy industrial factories) to improve the air-quality for the past two decades. In this study, effect of afforestation on reducing the  $\text{NO}_x$  concentration is investigated numerically using RAMS-HYPACT model.

**Key words:** Mountain-slope afforestation,  $\text{NO}_x$  concentration, RAMS-HYPACT, air pollution index, mountain-breeze circulation, stable stratification, inversion

## 1. Introduction

Lanzhou is an industrial city located at a narrow (2-8 km width), long (40-km), northwest-southeast oriented valley basin (elevation: approximately 1,500-m) with the Tibetan Plateau in the west, Baita mountain (above 1,700-m elevation) in the north, and the Gaolan mountain (above 1,900-m elevation) in the south (Fig. 1a). The aspect ratio of the valley (depth versus width) is around 0.07. Lanzhou contains four districts (Fig. 1b): Chengguan, Qilihe, Xigu, and Anning. Chengguan (District-I), located in the eastern valley, is the metropolitan area including government, commerce, culture, and residence. Xigu (District-III), located in the western valley, is the large heavy industrial area. Qilihe (District-II), located in the middle valley, and Anning (District-IV), located in the north middle valley, are the mixed residential, small factories, and farming (vegetables) area.

Annual and daily mean air quality criteria for urban areas generated by the State Environmental Protection Agency (SEPA) are used as the air quality standards. In Lanzhou, the second level criterion is taken for the commercial and residential regions and the third level criterion is taken for the industrial regions. For ( $\text{NO}_x$ ,  $\text{NO}_2$ ) pollutants, the annual mean second-level and third-level criteria are (0.05, 0.04  $\text{mg m}^{-3}$ ) and (0.10, 0.08  $\text{mg m}^{-3}$ ) (Table 1). The daily mean second-level and third-level criteria are (0.10, 0.08  $\text{mg m}^{-3}$ ) and (0.15, 0.12  $\text{mg m}^{-3}$ ) (Table 2). As the concentration is higher than the second-level air-quality criteria, the local SEPA will give the air-pollution alert.

An air-quality monitoring system has been established in Lanzhou with multiple sampling and sufficient numbers of stations. This monitoring system is the part of the project entitled Air Pollution and Control in Lanzhou (APCL), supported jointly by Gansu Province and the Chinese Academy of Sciences and carried out from 1999 to 2001.

Fig. 2 shows the spatial distribution of annual  $\text{NO}_x$  emission rate per square kilometer (unit:  $10^3 \text{ kg km}^{-2} \text{ yr}^{-1}$ ) in 2000. District-I (commercial and residential) and District-3 (industrial) (indicated with 'H' in Fig. 2). The special topographic features of Lanzhou metropolitan area block the air streams due to the large frictional forces and causes weak winds. In the winter, the occurrence of the calm winds is nearly 80%. In the evening (occasionally even in the daytime) low-level inversion exists to inhibit turbulent diffusion. These factors cause Lanzhou the one of the most polluted cities in China.

Since mid 1990s, the local Lanzhou government has conducted afforestation on the mountain slope and shut down several factories that emitted large amount of pollutants. The gaseous pollutants such as  $\text{NO}_x$  have been reduced. Fig. 3 shows the evolution of annual mean concentration for  $\text{NO}_x$  measured at the SEPA station ( $103.631^\circ\text{E}$ ,  $36.103^\circ\text{N}$ ), which is marked as the solid circle in Fig. 1b. The annual mean  $\text{NO}_x$  has two maxima (above the third level standard:  $0.10 \text{ mg m}^{-3}$ ) in 1990 and 1995, and decreases monotonically to  $0.05 \text{ mg m}^{-3}$  (close to the second level standard:  $0.05 \text{ mg m}^{-3}$ ) in 2000 (Fig. 3).

The purpose of this study is to investigate the effect of afforestation on the reduction of NO<sub>2</sub> and NO<sub>x</sub> pollutions in Lanzhou metropolitan area. First, we analyze temporal and spatial variability of NO<sub>2</sub> and NO<sub>x</sub> pollutions observed in 2000 is analyzed. Second, coupled Regional Atmospheric Modeling System (RAMS) and Hybrid Particle and Concentration Transport Model (HYPACT) [Tripoli and Cotton, 1982; Pielke Sr., et. al., 1992] are used to study the effect of afforestation. Two numerical experiments are conducted with the same boundary and initial conditions except for the land surface without (control run) and with (sensitivity run) afforestation. The model differences on the atmospheric conditions and NO<sub>x</sub> concentration are analyzed.

## **2. Data**

### **2.1. Concentration**

NO<sub>2</sub> and NO<sub>x</sub> monitoring system has been established in Lanzhou with multiple sampling and sufficient numbers of stations. This is the part of APCL, supported jointly by Gansu Province and the Chinese Academy of Sciences and carried out from 1999 to 2001. From the APCL project, the air quality data were collected at observational stations (St-1 - St-5) from October 1999 to April 2001 and at observational stations (St-6 - St-8) from August 2000 to April 2001. Over these stations, daily NO<sub>2</sub> and NO<sub>x</sub> concentrations are calculated. Table 3 shows the geography of the stations and the temporal averages of NO<sub>x</sub> concentration in 2000 (January – December for station-1 to station-5 and August – December for station-6 to station-8). Station-5 (Yuzhong),

located in a clean countryside, is taken as the reference station, where the annual mean  $\text{NO}_x$  concentrations is less than the first-level national air quality criteria (comparison between Table 3 and Table 1).

Fig. 4 shows the temporal variation of daily mean  $\text{NO}_x$  concentrations at four APCL stations (St-1, St-3, St-4, and St-7) to represent District-I, District-II, District-III, and District-IV, respectively. The horizontal dashed and solid lines are referred to as the second and third level criteria for daily mean concentrations (Table 2). The  $\text{NO}_x$  concentration of the four stations is lower than the second level criterion ( $0.10 \text{ mg m}^{-3}$ ) all the time from February to September except few occasions. However, the  $\text{NO}_x$  concentration exceeds the second level standard from October to January (winter) almost all the time. Station-4 (District-III) has the most series  $\text{NO}_x$  pollution problem during the periods from October 1999 to January 2000 and from October 2000 to April 2001. The daily mean  $\text{NO}_x$  concentration usually exceeds the second-level criterion ( $0.10 \text{ mg m}^{-3}$ ), and even exceeds the third-level criterion ( $0.15 \text{ mg m}^{-3}$ ). The annual mean  $\text{NO}_x$  concentrations are (0.06, 0.05, 0.06, 0.05) at St-1, St-3, St-4, and St-7 (Table 3). These values are all great than or equal to the second-level criterion for annual mean  $\text{NO}_x$  concentration ( $0.05 \text{ mg m}^{-3}$ ) (Table 1).

## **2.2. Air Pollution Index**

Air pollution index (API) is a quantitative measure for uniformly reporting the air quality for different constituents and connects to the human health. SEPA classifies the air quality standards into 5 major categories due to API values (Table 4): I (clean), II

(good), III (low-level pollution), IV (mid-level pollution), and V (high-level pollution).

The categories III and IV have two sub-categories: (III<sub>1</sub>, III<sub>2</sub>) and (IV<sub>1</sub>, IV<sub>2</sub>).

Daily mean API of NO<sub>x</sub> at St-E (its location see Fig. 1b) shows an evident seasonal variation with larger values (maximum around 200) in winter (low-level pollution, Category-III) and much smaller values (usually smaller than 100) in other seasons. Monthly mean API of NO<sub>x</sub> shows the similar seasonal variability with larger value in winter and much smaller value in other seasons (Fig. 5).

### **2.3. Long Term Trend**

The long-term variation of the annual mean NO<sub>x</sub> concentration shows the following features during 1988-2000 (Fig. 3). The second-level and third-level criteria of the annual mean are represented by dotted-dashed and dotted horizontal lines. The annual mean NO<sub>x</sub> concentration generally varies between the second-level and third-level criteria (see Table 1) except 1990 (0.106 mg m<sup>-3</sup>), 1995 (0.103 mg m<sup>-3</sup>) (higher than higher than the third-level criterion) and 1988 (0.046 mg m<sup>-3</sup>, lower than the second-level criterion). NO<sub>x</sub> has an evident decreasing trend (with time) since 1995. Reduction of NO<sub>x</sub> concentration since mid 1990s is due to the effort of the local Lanzhou government on the mountain-slope afforestation and on the closure of several factories that emitted large amount of pollutants.

## **3. Numerical Modeling**

Effect of mountain slope afforestation on reducing winter NO<sub>x</sub> pollution in Lanzhou is investigated using the coupled RAMS-HYPACT model.

### **3.1. RAMS**

Non-hydrostatic RAMS-4.3 [Pielke et al., 1992] is used in this study. The horizontal grid uses a rotated polar-stereographic projection. The vertical structure of the grid uses terrain-following coordinate system. The top of the model domain is flat and the bottom follows the terrain [Tripoli and Cotton, 1982]. The standard Arakawa C grid is used. RAMS contains lots of physics processes such as turbulent mixing [Helfand and Labraga, 1988], long and short-wave radiation [Chen and Cotton, 1987], wet physics describing the interaction among the cloud formation and the liquid, solid precipitation materials, the sensible and latent heat exchange between the atmosphere and multi-layer soil, surface vegetation and surface water, topographic dynamic affection and cumulus convection parameterization. In the numerical simulation, a flat bottom with elevation of 1460 m is assumed. This indicates that 850 hPa level is nearly at the land surface. See the RAMS website: <http://www.rams.atmos.colostate.edu> for more information.

### **3.2. HYPACT**

HYPACT was developed to simulate the motion of atmospheric tracers such as surface deposition, evaporation and condensation, precipitation scavenging, and other complex physical and chemical interactions under the influence of winds and atmospheric turbulence [Walko et al., 2001]. It adopts mixed Lagrangian and Eulerian approaches [Hurley and Physick, 1993]. The Eulerian system in HYPACT is similar to RAMS: a scalar field is predicted with advection and diffusion. For small scale

pollutant air mass during the initial state, the tiny-grid Lagrangian component represents sources with any size and maintenance of concentrated, narrow pollutant plumes until being broadened by atmospheric dispersion. The position of SO<sub>2</sub> plume is described by

$$\begin{aligned}X(t + \Delta t) &= X(t) + (u + u')\Delta t \\Y(t + \Delta t) &= Y(t) + (v + v')\Delta t \\Z(t + \Delta t) &= Z(t) + (w + w')\Delta t\end{aligned}$$

where  $(u, v, w)$  are the three-dimensional grid-scale wind components; and  $(u', v', w')$  are three-dimensional sub-grid scale (turbulence) wind components.

When the SO<sub>2</sub> plume becomes large enough to be recognized by the Eulerian system, the Eulerian method is used. The Lagrangian pollutant plume can be converted into a concentration field and then advected using an Eulerian formulation. The location and concentration of NO<sub>x</sub> plume is predicted by HYPACT using meteorological output from the RAMS. While a purely Eulerian treatment for the calculation of NO<sub>x</sub> concentration using the RAMS is possible, the HYPACT module offers an alternative method for estimating atmospheric transport and dispersion that is not restricted by the spatial resolution of the RAMS model.

### **3.3. Boundary and Initial Conditions**

At the surface, we use USGS vegetation 25-category with type-1 for urban/built-up land, and type-4 for mixed dry/irrigational plants. Afforestation is the type-4 used for the mountain slope (Fig. 6). When type-4 is replaced by type-1 on the mountain-slope, it reduces to the non-afforestation case. The NCEP data along the lateral boundary (every 6 hours) of the largest box from December 1 to 31, 2000 are

taken as the open boundary condition. One way nesting is used for the triple-nested grid system. The larger model provides the lateral boundary conditions for the smaller model using a 5 point-buffer zone. The NCEP reanalysis data on December 1, 2000 are taken as the initial condition. The atmosphere is at rest ( $\mathbf{V} = 0$ ) with horizontally uniform temperature and specific humidity soundings, which are taken from NCEP reanalyzed data for Lanzhou at 00 GMT [0700 Beijing time (BT)] on December 1, 2000. RAMS is integrated from the initial conditions with the temporally varying solar irradiance at the top of the atmosphere since December 1, 2000.

Using RAMS multiple grid nested scheme, the model equations are solved simultaneously on any number of interacting computational meshes of differing spatial resolution. The time dependent model solution is first updated on the coarsest grid. A tri-quadratic spatial interpolation is then performed to obtain values that are assigned to the spatial boundaries of a finer grid nested within a coarser grid. The model fields on the finer grid are then updated using the coarser grid interpolated values as the spatial boundary conditions. Once the finer grid is at the same time level as the coarser grid, local spatial averages of the fine grid fields are obtained and used to overlay the coarse grid fields. The two-way interaction between the nested grids is performed following the scheme by Clark and Hall [1991] and Walko et al. [1995].

Five nested grids and 25 vertical levels illustrated by Chu et al. [2005] are used. The vertical spacing is 200 m near the surface and increases to 800 m above 2400 m. The vertical grid structure is the same for all five nested grids. The outer grid (Grid-1) was a  $40 \times 30$  grid with a horizontal resolution of 54 km and a time step of 90 s. The first

nested grid (Grid-2) was a  $38 \times 29$  grid with a horizontal resolution of 18 km and a time step of 30 s. The second nested grid (Grid-3) was a  $38 \times 29$  grid with a horizontal resolution of 6 km and a time step of 10 s. The third nested grid (Grid-4) was a  $38 \times 29$  grid with a horizontal resolution of 2 km and a time step of  $10/3$  s. The innermost grid (Grid-5) was a  $62 \times 42$  grid with a horizontal resolution of 1 km and a time step of  $5/3$  s. The first three grid systems (grid-1 to grid-3) are centered at ( $103.8^\circ\text{E}$ ,  $36.06^\circ\text{N}$ ). The last two grid systems (grid-4 to grid-5) are centered at ( $103.8^\circ\text{E}$ ,  $36.08^\circ\text{N}$ ). Using this configuration enables the influence of relatively fine-scale topographic flows on ash dispersal and deposition to be assessed. After integrating RAMS model, the meteorological variables are inputted into HYPACT every hour.

### **3.4. $\text{NO}_x$ Pollution Sources**

Pollution sources can be flexibly set in HYPACT as single or multiple, instantaneous, continuous, or time varying. The source geometry can be point, line, area, or volume with various orientations, based on the spatial dimensions and the shape of horizontal section of the actual pollution sources. Since only the total amount of  $\text{NO}_x$  emission in 2000,  $A(x, y)$ , is available (see Fig. 2), the  $\text{NO}_x$  emission rate is the temporal mean over the year.

### **3.5. Model Capability**

Model capability of RAMS-HYPACT for predicting air pollution in Lanzhou can be verified using the observational data collected by the APCL air-quality monitoring system from August 2000 to April 2001. Here, the  $\text{NO}_x$  plume spreading and enhancing event from 0700 BT on Dec 11 to 0700 BT on Dec 12, 2000 is taken as illustration.

Fig. 7 shows temporally varying sounding (from 0200 BT to 2100 BT on Dec 11, 2000) averaged horizontally over the inner most grid area (Grid-5) predicted by RAMS. Below 2000-m height, the lapse rate ( $\gamma = -\partial T / \partial z$ ) during the evening (0200 BT, 0600 BT, 2100 BT) has evident low-level inversion between 1700-m and 1850-m. The daytime (1700 BT, three hours after the local noon time) sounding (Fig. 7c) shows a linear lapse rate with the temperature decreasing from 3.0°C at 1520-m to -2°C at 2150-m ( $\gamma = 0.79^\circ\text{C}/100\text{ m}$ ). Since the dry-adiabatic lapse rate ( $\Gamma$ ) is  $0.98^\circ\text{C}/100\text{ m}$ , the simulated lapse rate in the air column 500 to 600 m above the ground on Dec 11, 2000 is always stable (day and night), i.e.,  $\gamma < \Gamma$ . The strong stratification reduces the diffusion of  $\text{NO}_x$  and increases the concentration when the pollutant emission rate keeps constant. The simulated mountain breeze circulation along 36.12°N latitude has downward motion along the mountain-slope. An upward branch is located at the middle of the valley on 0700 BT on Dec 11, 2000 (Fig. 8a). Such a strong upward branch may cause local low  $\text{NO}_x$  concentration. Therefore, two  $\text{NO}_x$  plumes (concentration  $> 0.1\text{ mg}/\text{m}^3$ ) occur at 0700 BT on Dec 11 (Fig. 9a) with low  $\text{NO}_x$  pollution (concentration  $< 0.1\text{ mg}/\text{m}^3$ ) in between, which is corresponding to the strong upward motion (Fig. 8a). The simulated mountain-breeze circulation at 0700 BT on Dec 12, 2000 (Fig. 8b) is quite different from that at 0700 BT on Dec 11, 2000 (Fig. 8a). The upward branch shifts eastward. The valley is mainly occupied by the downward flow, which suppresses the upward transport of  $\text{NO}_x$  pollutant, and causes low-level high  $\text{NO}_x$  concentration spreading (Fig. 9b). The increase of the low-level  $\text{NO}_x$  concentration was also observed from Dec

11 to Dec 12, 2000 (Fig. 10). The maximum  $\text{NO}_x$  concentration (in the east part of Lanzhou) increases from  $55 \mu\text{g m}^{-3}$  on Dec 11 to  $75 \mu\text{g m}^{-3}$  on Dec 12.

#### **4. Effect of Afforestation**

Thermal heterogeneity of land surface can produce local circulations as strong as sea breezes [e.g., Chu 1987, 1989]. Differential surface heating on the mountain slope generates downward mountain winds in winter or night. The downward motion over the valley makes the atmosphere very stable (even inversion), and in turn weakens the diffusion of the pollutants. Weakening this mountain-valley circulation (strong downward branch over the valley) destabilizes the atmosphere and enhances the diffusion rate. From physical point of view, reduction of surface thermal heterogeneity will weaken this circulation. Afforestation on the mountain slope may reduce the thermal heterogeneity and in turn improve the air-quality by atmospheric destabilization.

The improvement of air quality due to afforestation is identified from comparison between two numerical experiments. Two numerical experiments are conducted with the same boundary and initial conditions except for the land surface without (control run) and with (sensitivity run) afforestation. The temporally mean  $\text{NO}_x$  concentrations are horizontally averaged for the two areas (Fig. 11): (a) Cheng Guan area (commercial and residential district) and (b) Xi Gu area (heavy industrial district). Thus, we have two vertical profiles of the  $\text{NO}_x$  concentration for each area. The  $\text{NO}_x$  concentration is evidently smaller with afforestation (Figs. 11a, d) than without afforestation (Figs. 11b, e) at all depths. The reduction of  $\text{NO}_x$  concentration is larger in Xi Gu area (maximum

reduction of  $22 \mu\text{g m}^{-3}$  located at about 400 m above the land surface) (Fig. 11f) than in Cheng Guan area (maximum reduction of  $12.5 \mu\text{g m}^{-3}$  located at about 250 m above the land surface) (Fig. 11e).

## 5. Conclusions

(1) Special topographic features of Lanzhou metropolitan area (narrow and long valley) block the air streams due to the large frictional forces and causes weak winds. In the winter, the occurrence of the calm winds is nearly 80%. In the evening (occasionally even in the daytime) low-level inversion exists to inhibit turbulent diffusion and in turn to cause heavy  $\text{NO}_x$  pollution.

(2) Observational and modeling studies show that the mountain-breeze circulation along with strongly stable stratification causes the  $\text{NO}_x$  plume formation. The location of the upward branch of the mountain-valley circulation controls the spreading of the  $\text{NO}_x$  plume. When the upward branch in the center of the valley, the  $\text{NO}_x$  plumes are separated by the upward branch since the upward branch transports the pollutants from low-level to high-level and reduces the low-level air pollution. When the upward branch moves out of the valley, the low-level  $\text{NO}_x$  plume spreads horizontally. With strong stratification, the  $\text{NO}_x$  plume strengthens.

(3) Mountain-slope afforestation reduces the thermal heterogeneity and in turn improves the air-quality by atmospheric destabilization. Such a mechanism is identified using numerical experiments with and without mountain-slope afforestation using RAMS-HYPACT. The simulated  $\text{NO}_x$  concentration is evidently (up to 40%) smaller

with afforestation than without afforestation at all depths. This work also shows the capability of the RAMS-HYPACT model in predicting air quality.

### **Acknowledgments**

This work was jointly supported by the National Natural Science Foundation of China Major Programs No. 40305020, and the Naval Postgraduate School. The data for this study are provided by the program entitled “Air Pollution and Control in Lanzhou” jointly sponsored by the local government of Gansu Province and the Chinese Academy of Science.

## References

- Chen, C., and Cotton W.R., 1987. The physics of the marine stratocumulus-capped mixed layer. *Bound. Lay. Meteor.*, 25, 289-321.
- Chu, P.C., 1987. An icebreeze mechanism for an ice divergence-convergence criterion in the marginal ice zone. *J. Phys. Oceanogr.*, 17, 1627-1632, 1987.
- Chu, P.C., 1989. Relationship between sea surface temperature gradient and thermally forced planetary boundary layer air flow. *Pure & Applied Geophys.*, 130, 31-45.
- Chu, P.C., S.H. Lu, and Y.C. Chen, 2005. A numerical modeling study on desert oasis self-supporting mechanism. *Journal of Hydrology*, 312, 256-276.
- Clark, T.L., and W.D. Hall, 1991. Multi-domain simulations of the time dependent Navier-Stokes equations: Benchmark error analysis of some nesting procedures. *J. Comput. Phys.*, 92, 456-481.
- Helfand, H. M., and J. C. Labraga, 1988. Design of a non-singular level 2.5 second-order closure model for the prediction of atmospheric turbulence. *J. Atmos. Sci.*, 45, 113–132.
- Hurley, P. J., and W. L. Physick, 1993. A skewed, homogeneous Lagrangian particle model for convective conditions. *Atmos. Environ.*, 27A, 619–624.
- Pielke, R. A., W. R. Cotton, R. L. Walko, C. J. Tremback, W. A. Lyons, L. D. Grasso, M. E. Nicholls, M. D. Moran, D. A. Wesley, T. J. Lee and J. H. Copeland, 1992. A comprehensive Meteorological Modeling system –RAMS, *Meteor. Atmos. Phys.*, 49, 69-91.
- Tripoli, G. J., and W. R. Cotton, 1982. The Colorado State University three-dimensional cloud/mesoscale model—1982. Part I: General theoretical framework and sensitivity experiments. *J. Rech. Atmos.*, 16, 185-219.
- Walko, R.L., C.J. Tremback, R.A. Pielke, and W.R. Cotton, 1995. An interactive nesting algorithm for stretched grids and variable nesting ratios. *J. Appl. Meteor.*, 34, 994-999.
- Walko, R.L., Tremback, C.J., Bell, M.J., 2001. HYPACT Hybrid Particle and Concentration Transport Model, User's Guide. Mission Research Corporation, Fort Collins, CO.

## Table Caption

Table 1. Air quality standards for annual mean  $\text{NO}_x$  and  $\text{NO}_2$  concentrations ( $\text{mg m}^{-3}$ ) from the Chinese National Environmental Protection Agency.

Table 2. Air quality standards for daily mean  $\text{NO}_x$  and  $\text{NO}_2$  concentrations ( $\text{mg m}^{-3}$ ) from the Chinese National Environmental Protection Agency.

Table 3. Location of observational stations and temporally total mean  $\text{NO}_x$  concentration ( $\text{mg m}^{-3}$ ) during the whole observational period. Note that the second-level annual mean criterion is  $0.05 \text{ mg m}^{-3}$  for  $\text{NO}_x$ .

Table 4. API and air quality management in China.

## Figure Captions

Figure 1: Lanzhou: (a) geography and (b) topography.

Figure 2. Spatial distribution of annual  $\text{NO}_x$  emission rate per square kilometer (unit:  $10^3 \text{ kg km}^{-2} \text{ yr}^{-1}$ ) in 2000. Here, the industrial sources are indicated with underlines; high-level sources are represented by the enclosed solid curves marked as 'H'. The dashed contours are topography (unit: m).

Figure 3. Annual mean  $\text{NO}_x$  concentration ( $\text{mg m}^{-3}$ ) measured at the local CEPA station ( $103.631^\circ\text{E}$ ,  $36.103^\circ\text{N}$ ), which is marked as the solid circle in Fig. 1b. The second-level criterion is represented by the horizontal dash-dotted line and the third-level criterion is represented by the horizontal dotted line.

Figure 4. Daily mean  $\text{NO}_x$  concentrations ( $\text{mg m}^{-3}$ ) at St-1, St-3, St-4 and St-7 representing four districts. Horizontal dashed line is daily mean second-level criterion, while horizontal solid line is daily mean third-level criterion.

Figure 5. Daily mean API of  $\text{NO}_2$  at station-E.

Figure 6. Experiment for mountain-slope afforestation. Note that the soil is use type-4 for the mountain slope. The soil type-4 is replaced by type-1 for the experiment without mountain-slope afforestation.

Figure 7. Model simulated and horizontally averaged temperature profiles over the grid-5 region (i.e., Lanzhou) on December 11, 2000: (a) 0200 BT, (b) 0600 BT, (c) 1700 BT (three hours after the local noon time), and (d) 2100 BT.

Figure 8. Model simulated mountain breeze circulation along  $36.12^\circ\text{N}$  latitude at (a) 0700 BT on Dec 11, 2000, and (b) 0700 BT on Dec 12, 2000.

Figure 9. Model simulated  $\text{NO}_x$  plume (concentration  $> 0.1 \text{ mg/m}^3$ ) spreading and enhancing from (a) 0700 BT, Dec 11 to (b) 0700 BT, Dec 12, 2000

Figure 10. Observed  $\text{NO}_x$  concentration on (a) December 11, and (b) December 12, 2000.

Figure 11. Two areas of interest: (a) XiGu (industrial district), and (b) Cheng Guan (commercial and residential district).

Figure 12. Temporally mean  $\text{NO}_x$  concentration for: (a) Cheng Guan Region without afforestation (Exp-1), (b) Cheng Guan Region with afforestation (Exp-2), (c) Cheng Guan Region  $\text{NO}_x$  reduction due to afforestation (Exp-2 minus Exp-1), (d) Xi Gu region without afforestation (Exp-1), (e) Xi Gu region with afforestation (Exp-1), (f) Xi Gu region  $\text{NO}_x$  reduction due to afforestation (Exp-2 minus Exp-1). Here, the vertical axis denotes the height about the land surface.

Table 1. Air quality standards for annual mean NO<sub>x</sub> and NO<sub>2</sub> concentrations (mg m<sup>-3</sup>) from the Chinese National Environmental Protection Agency.

Level of Criterion	NO <sub>x</sub>	NO <sub>2</sub>
1	0.03	0.02
2	0.05	0.04
3	0.10	0.08

Table 2. Air quality standards for daily mean NO<sub>x</sub> and NO<sub>2</sub> concentrations (mg m<sup>-3</sup>) from the Chinese National Environmental Protection Agency.

Level of Criterion	NO <sub>x</sub>	NO <sub>2</sub>
1	0.05	0.04
2	0.10	0.08
3	0.15	0.12

Table 3. Location of observational stations and temporally total mean NO<sub>x</sub> concentration (mg m<sup>-3</sup>) during the whole observational period. Note that the second-level annual mean criterion is 0.05 mg m<sup>-3</sup> for NO<sub>x</sub>.

Site	Longitude E	Latitude N	Height Above Surface (m)	Region	NO <sub>x</sub>
St-1	103.84	36.04	25	Chengguan (District-1)	0.06
St-2	103.84	36.07	11	Chengguan (District-1)	0.04
St-3	103.71	36.08	15	Qilihe (District-3)	0.05
St-4	103.63	36.10	22	Xigu (District-2)	0.06
St-5	104.09	35.84	4	Yuzhong County	0.01
St-6	103.92	36.04	19	Chengguan (District-1)	0.03
St-7	103.74	36.10	15	Anning (District-4)	0.05
St-8	103.63	36.09	4	Xigu (District-2)	0.05

Table 4. API and air quality management in China.

Air Pollution Index	Air Quality Classification		Air Quality Description and Management
$API \leq 50$	I	Clean	No action is needed.
$50 < API \leq 100$	II	Good	No action is needed.
$100 < API \leq 150$	III <sub>1</sub>	Low-level pollution	Persons should be careful in outdoor activities.
$150 < API \leq 200$	III <sub>2</sub>		
$200 < API \leq 250$	IV <sub>1</sub>	Mid-level pollution	Persons with existing heart or respiratory illnesses are advised to reduce physical exertion and outdoor activities.
$250 < API \leq 300$	IV <sub>2</sub>		
$API \geq 300$	V	High-level pollution	Air pollution is severe; The general public is advised to reduce physical exertion and outdoor activities.

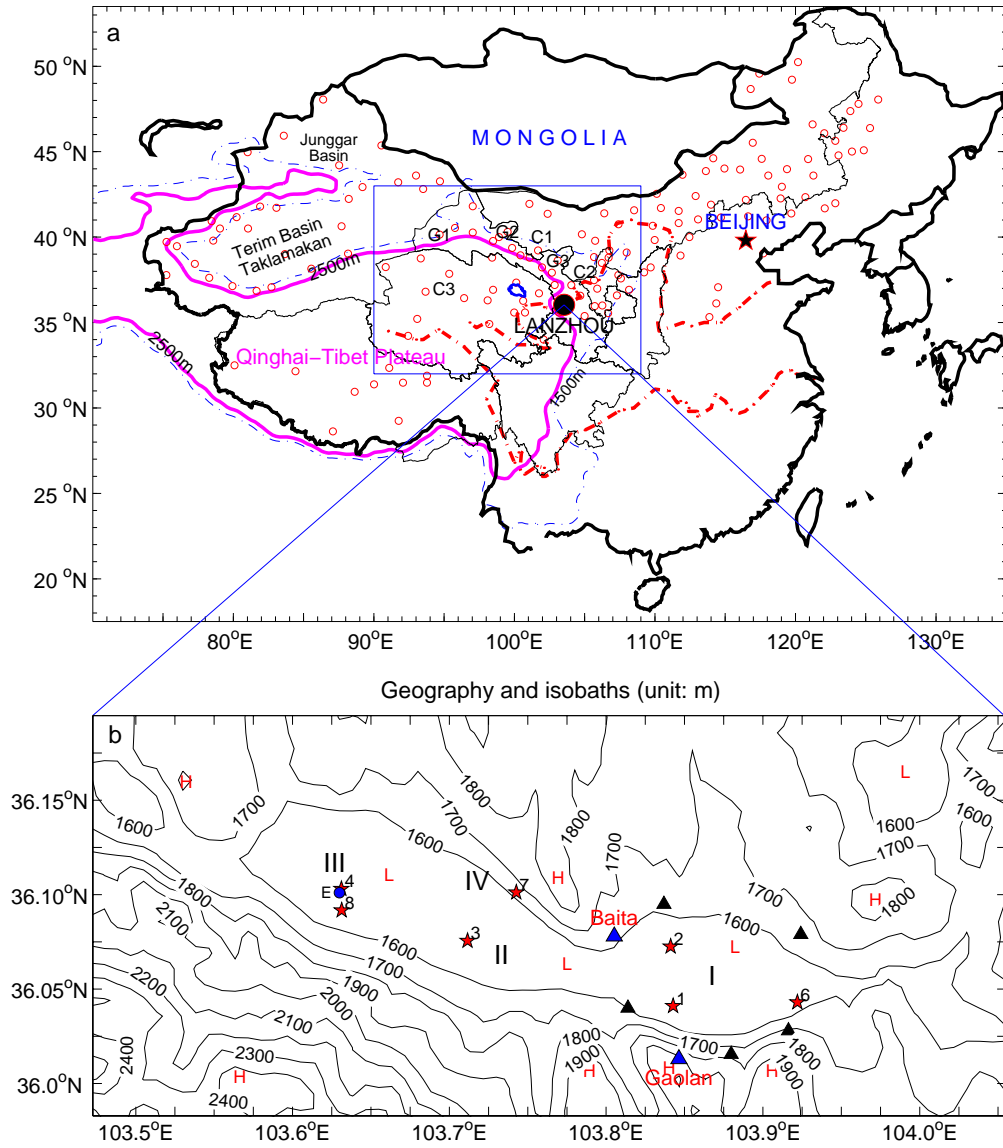


Figure 1: Lanzhou: (a) geography and (b) topography.

The NO<sub>x</sub> in 2000(1000kg)

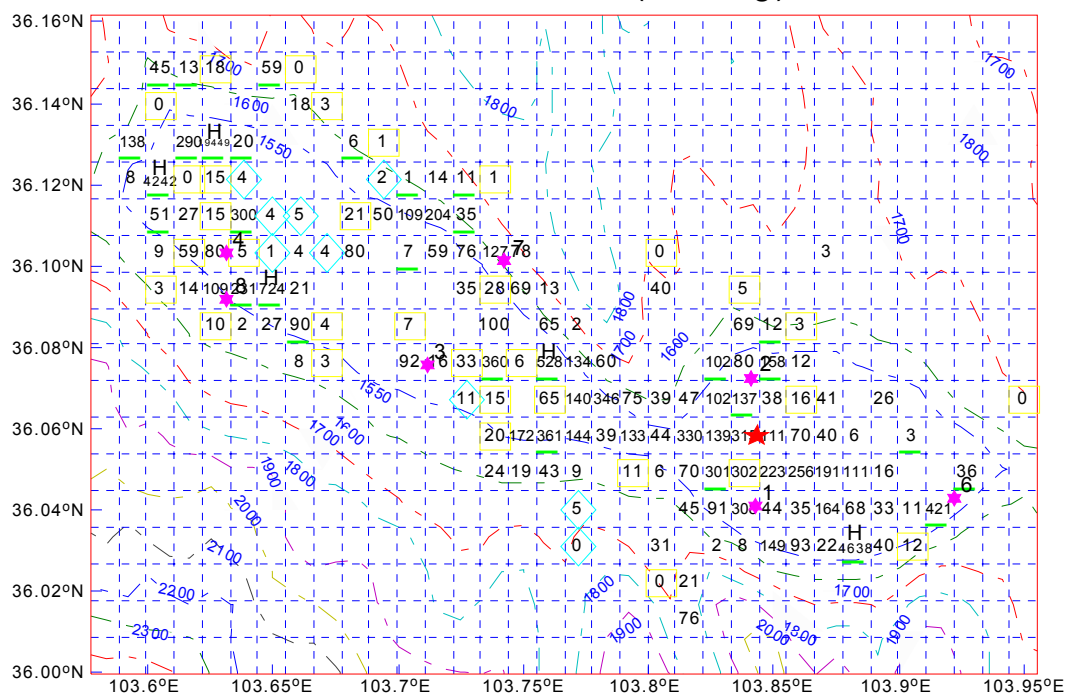


Figure 2. Spatial distribution of annual NO<sub>x</sub> emission rate per square kilometer (unit:  $10^3 \text{ kg km}^{-2} \text{ yr}^{-1}$ ) in 2000. Here, the industrial sources are indicated with underlines; high-level sources are represented by the enclosed solid curves marked as ‘H’. The dashed contours are topography (unit: m).

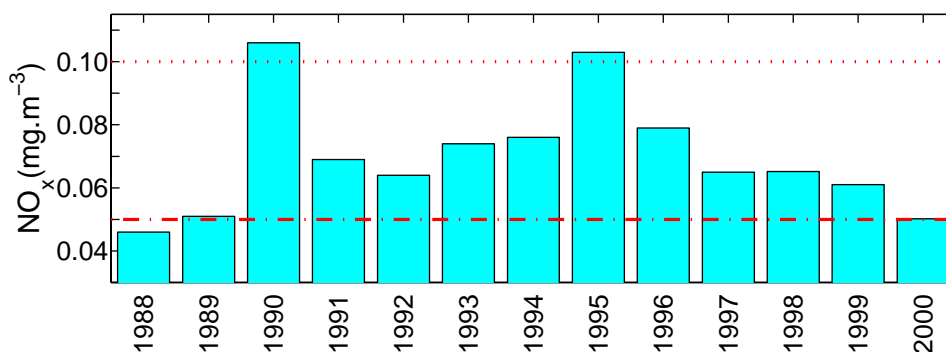


Figure 3. Annual mean NO<sub>x</sub> concentration ( $\text{mg m}^{-3}$ ) measured at the local CEPA station (103.631°E, 36.103°N), which is marked as the solid circle in Fig. 1b. The second-level criterion is represented by the horizontal dash-dotted line and the third-level criterion is represented by the horizontal dotted line.

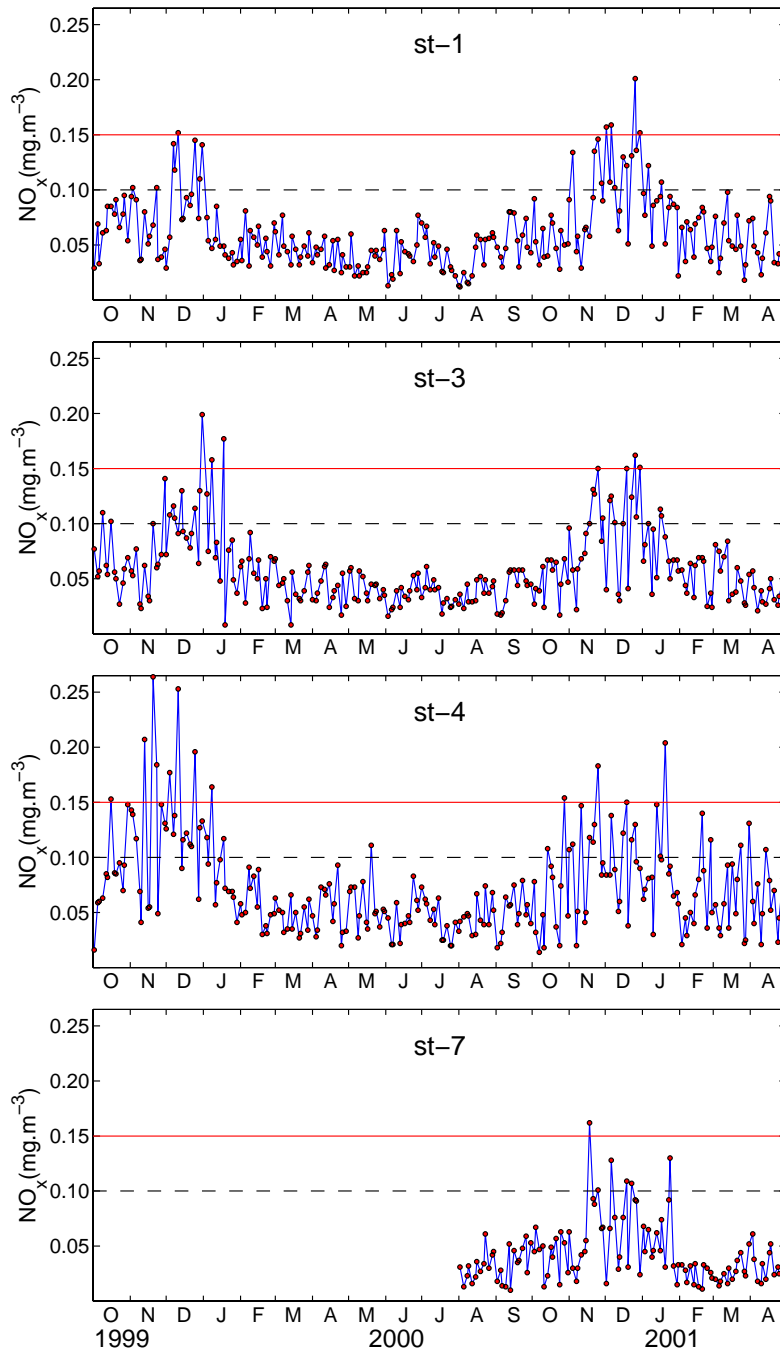


Figure 4. Daily mean  $\text{NO}_x$  concentrations ( $\text{mg m}^{-3}$ ) at St-1, St-3, St-4 and St-7 representing four districts. Horizontal dashed line is daily mean second-level criterion, while horizontal solid line is daily mean third-level criterion.

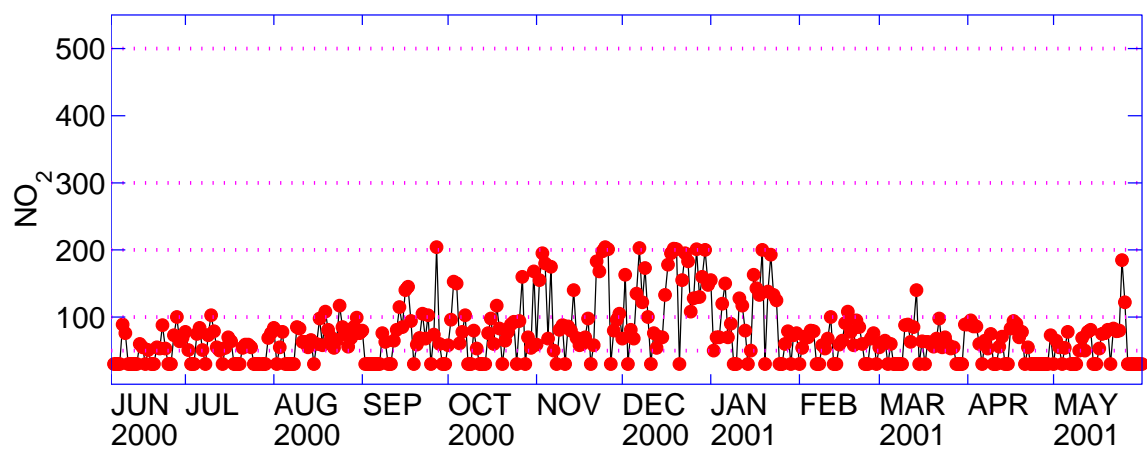


Figure 5. Daily mean API of NO<sub>2</sub> at station-E.

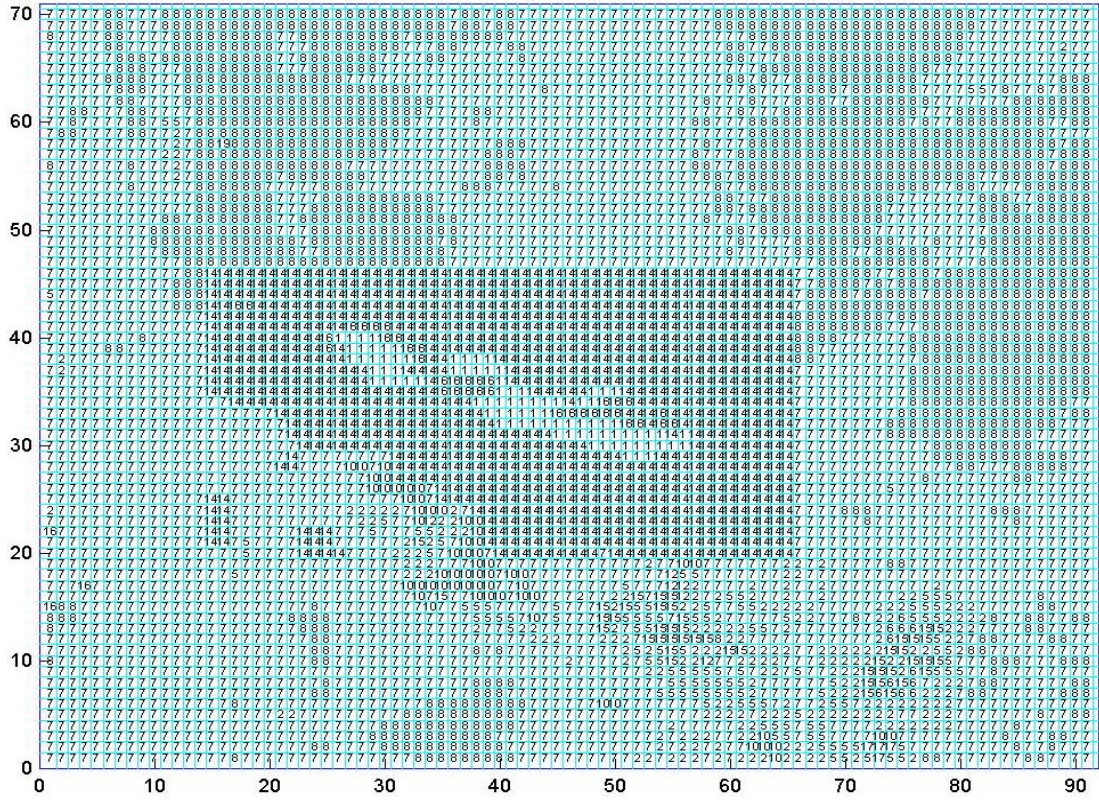


Figure 6. Experiment for mountain-slope afforestation. Note that the soil is use type-4 for the mountain slope. The soil type-4 is replaced by type-1 for the experiment without mountain-slope afforestation.

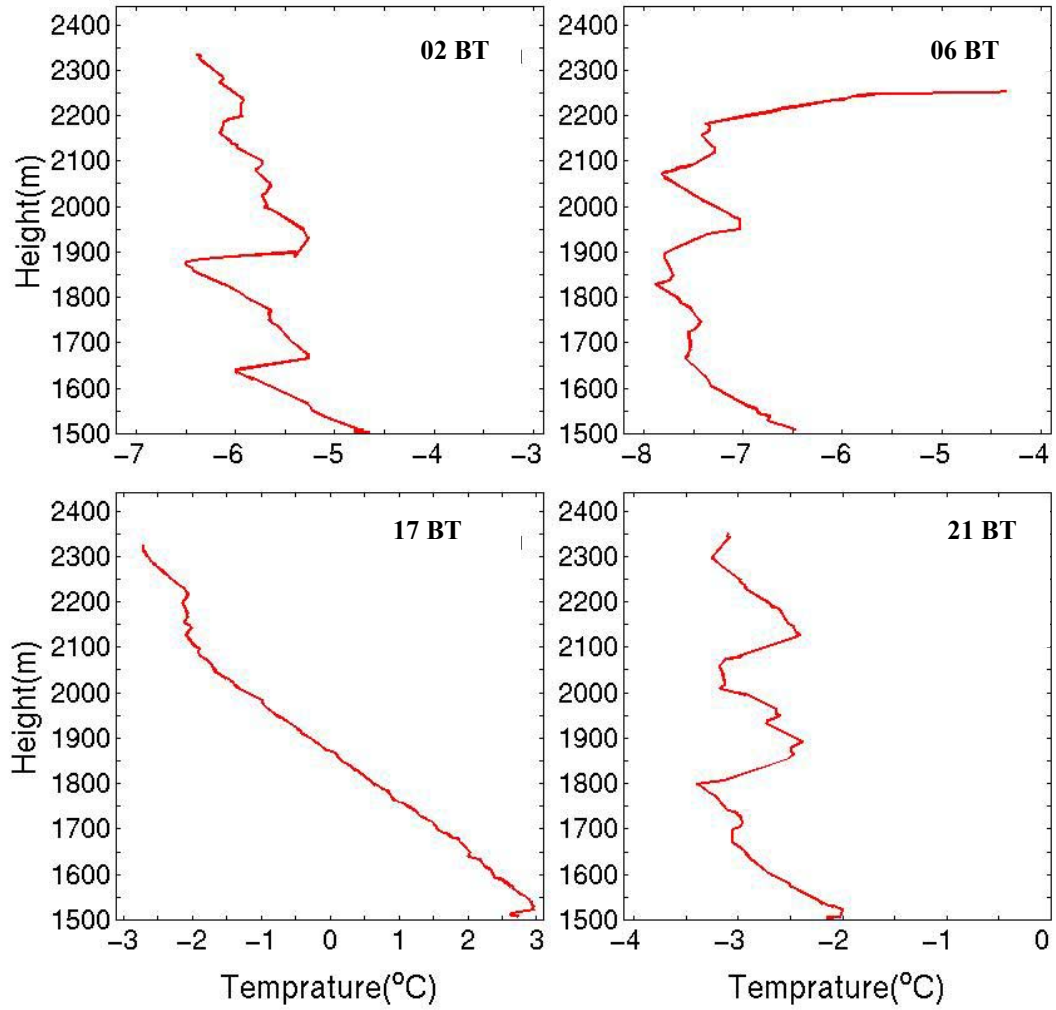


Figure 7. Model simulated and horizontally averaged temperature profiles over the grid-5 region (i.e., Lanzhou) on December 11, 2000: (a) 0200 BT, (b) 0600 BT, (c) 1700 BT (three hours after the local noon time), and (d) 2100 BT.

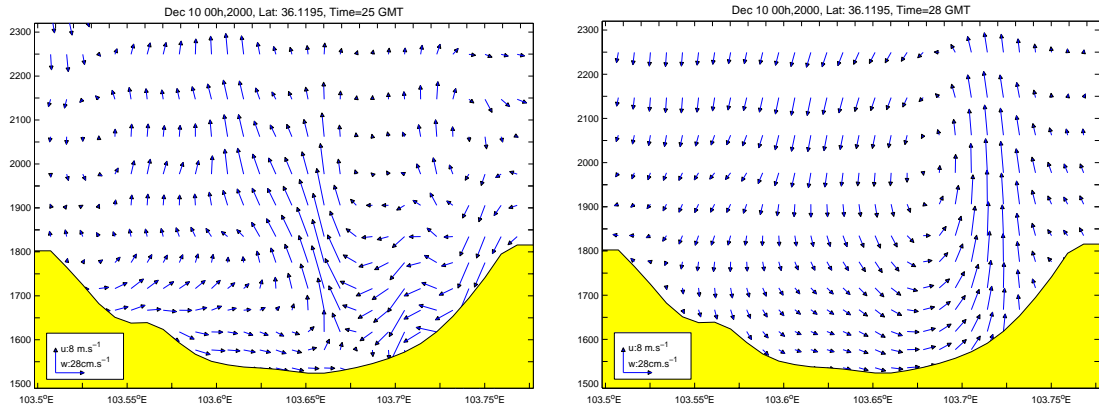


Figure 8. Model simulated mountain breeze circulation along 36.12°N latitude at (a) 0700 BT on Dec 11, 2000, and (b) 0700 BT on Dec 12, 2000.

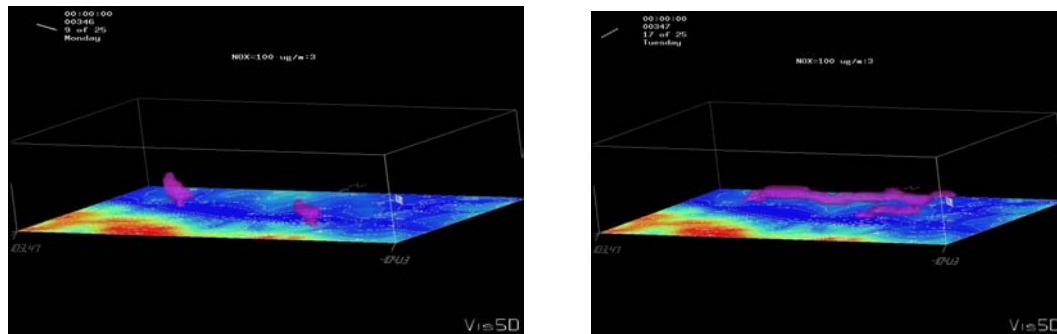


Figure 9. Model simulated NO<sub>x</sub> plume (concentration > 0.1 mg/m<sup>3</sup>) spreading and enhancing from (a) 0700 BT, Dec 11 to (b) 0700 BT, Dec 12, 2000.

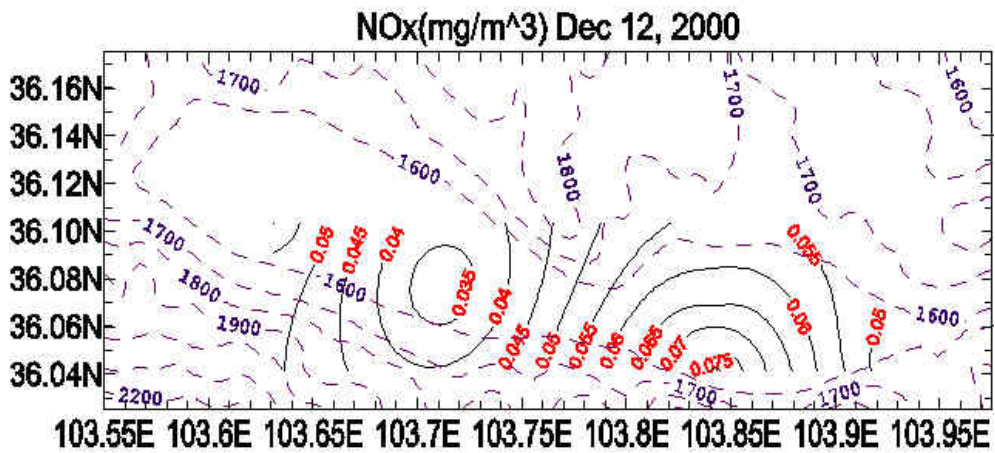
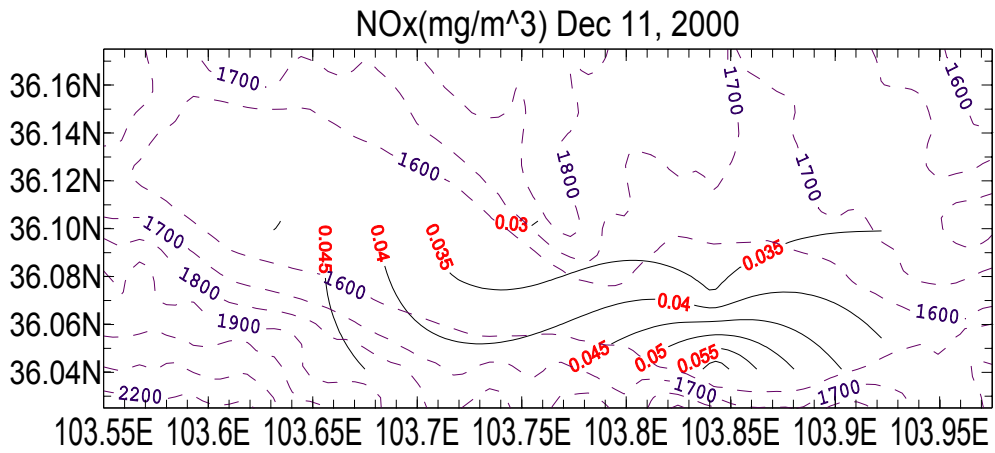


Figure 10. Observed NO<sub>x</sub> concentration on (a) December 11, and (b) December 12, 2000.

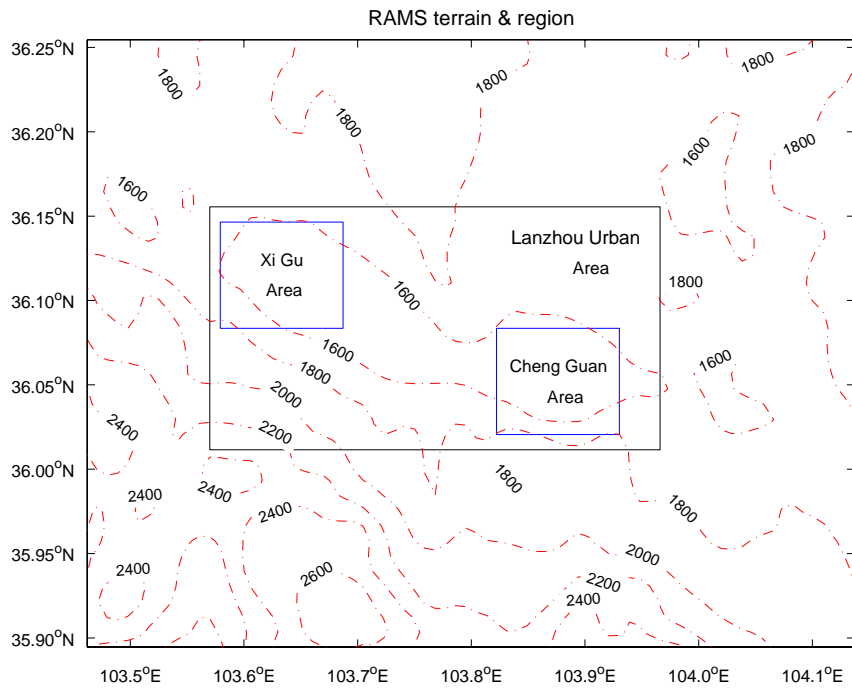


Figure 11. Two areas of interest: (a) XiGu (industrial district), and (b) Cheng Guan (commercial and residential district).

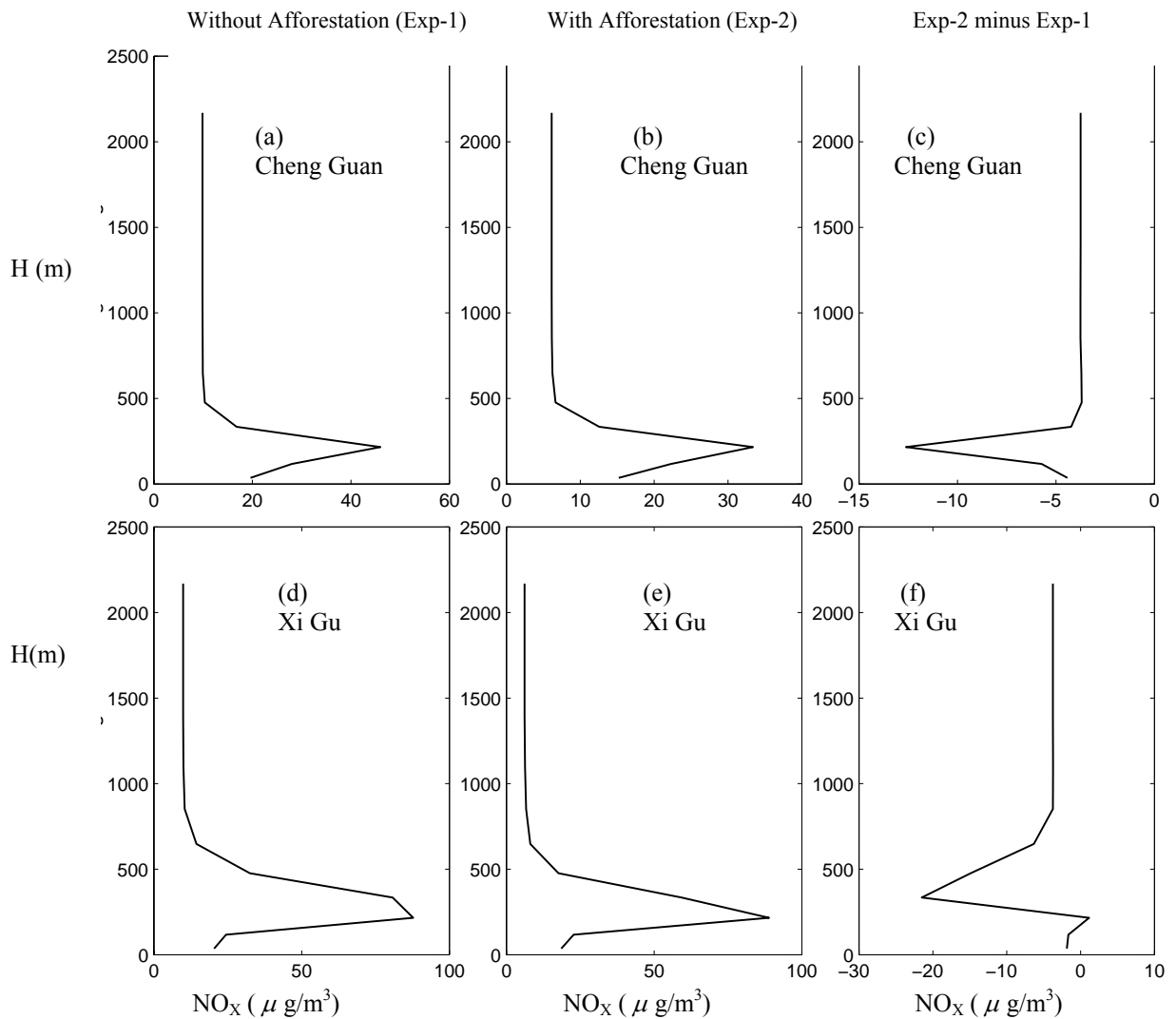


Figure 12. Temporally mean  $\text{NO}_x$  concentration for: (a) Cheng Guan Region without afforestation (Exp-1), (b) Cheng Guan Region with afforestation (Exp-2), (c) Cheng Guan Region  $\text{NO}_x$  reduction due to afforestation (Exp-2 minus Exp-1), (d) Xi Gu region without afforestation (Exp-1), (e) Xi Gu region with afforestation (Exp-1), (f) Xi Gu region  $\text{NO}_x$  reduction due to afforestation (Exp-2 minus Exp-1). Here, the vertical axis denotes the height about the land surface.

